Electronic Supplementary Information

Extended three-dimensional supramolecular architectures derived from trinuclear (bis-*β*-diketonato)copper(II) metallocycles

Jack K. Clegg,[a] **Leonard F. Lindoy,**[*a] **John C. McMurtrie**[a,b] **and David Schilter**[a]

[a] *Centre for Heavy Metals Research, School of Chemistry, University of Sydney, NSW 2006, Australia*

[b] *School of Physical and Chemical Sciences, Queensland University of Technology, GPO Box 2434, Brisbane 4001, Australia*

X-ray structure determinations

Specific details for $[Cu_3(L^2)_3] \cdot 0.5H_2O$

The hydrogen atoms on the water molecules could not be located in the Fourier difference map and were not modelled. A suitable model for disordered propyl groups could not be found and as such were modelled anisotropically without multiple positions for each atom. This resulted in larger than ideal U_{eq} min/max ratios.

Table S1. Selected Bond Lengths (Å) and Angles (°) for $[Cu_3(L^2)_3]0.5H_2O$

Cu(1)-O(12)	1.914(2)	Cu(2)-O(5)	1.914(2)
Cu(1)-O(1)	1.923(2)	Cu(3)-O(10)	1.908(2)
Cu(1)-O(11)	1.934(2)	Cu(3)-O(9)	1.916(2)
Cu(1)-O(2)	1.938(2)	Cu(3)-O(8)	1.919(2)
Cu(1)-O(2)^i	2.513(2)	Cu(3)-O(7)	1.928(2)
Cu(2)-O(4)	1.903(2)	O(2)-Cu(1)^i	2.513(2)
Cu(2)-O(3)	1.911(2)	Cu(2)-O(6)	1.912(2)
O(12)-Cu(1)-O(1)	86.18(9)	O(11)-Cu(1)-O(2)^i	89.32(8)
O(12)-Cu(1)-O(11)	93.13(9)	O(2)-Cu(1)-O(2)^i	85.44(8)
O(1)-Cu(1)-O(11)	172.13(9)	O(4)-Cu(2)-O(3)	93.02(9)
O(12)-Cu(1)-O(2)	176.93(9)	O(4)-Cu(2)-O(6)	175.29(10)
O(1)-Cu(1)-O(2)	92.37(8)	O(3)-Cu(2)-O(6)	86.27(9)
O(11)-Cu(1)-O(2)	87.93(8)	O(4)-Cu(2)-O(5)	87.31(9)
O(12)-Cu(1)-O(2)^i	97.44(8)	O(3)-Cu(2)-O(5)	174.68(10)
O(1)-Cu(1)-O(2)i	98.54(8)	O(6)-Cu(2)-O(5)	93.82(9)
O(10)-Cu(3)-O(9)	93.60(9)	O(10)-Cu(3)-O(8)	178.08(9)
O(9)-Cu(3)-O(7)	178.09(10)	O(9)-Cu(3)-O(8)	88.25(9)
O(8)-Cu(3)-O(7)	92.41(9)	O(10)-Cu(3)-O(7)	85.73(9)

^{i} Symmetry Code: $-x+2, -y+2, -z+2$
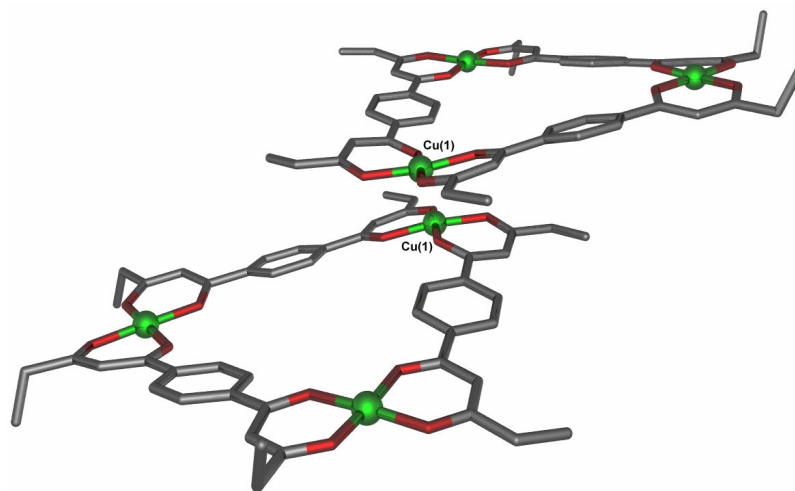
Figure S1. A schematic representation of the close packing in $[Cu_3(L^2)_3]\cdot 0.5H_2O$

Cu(3)-O(8)	1.942(2)	Cu(2)-O(1T)	2.461(4)
Cu(3)-N(2)[i]	2.373(3)	Cu(3)-O(10)	1.934(2)
N(2)-Cu(3)[ii]	2.373(3)	Cu(3)-O(9)	1.940(2)
O(11)-Cu(1)-O(12)	92.63(9)	O(4)-Cu(2)-O(5)	87.13(11)
O(11)-Cu(1)-O(2)	86.23(9)	O(6)-Cu(2)-O(5)	92.55(11)
O(12)-Cu(1)-O(2)	171.25(10)	O(3)-Cu(2)-O(1T)	97.80(13)
O(11)-Cu(1)-O(1)	173.33(10)	O(4)-Cu(2)-O(1T)	98.20(14)
O(12)-Cu(1)-O(1)	87.55(10)	O(6)-Cu(2)-O(1T)	92.14(12)
O(2)-Cu(1)-O(1)	92.58(9)	O(5)-Cu(2)-O(1T)	85.73(14)
O(11)-Cu(1)-N(1)	91.13(10)	O(10)-Cu(3)-O(9)	92.35(10)
O(12)-Cu(1)-N(1)	96.35(10)	O(10)-Cu(3)-O(7)	87.67(9)
O(2)-Cu(1)-N(1)	92.35(10)	O(9)-Cu(3)-O(7)	173.36(11)
O(1)-Cu(1)-N(1)	95.47(10)	O(10)-Cu(3)-O(8)	173.28(10)
O(3)-Cu(2)-O(4)	93.50(11)	O(9)-Cu(3)-O(8)	86.39(10)
O(3)-Cu(2)-O(6)	86.17(10)	O(7)-Cu(3)-O(8)	92.82(10)
O(4)-Cu(2)-O(6)	169.60(13)	O(10)-Cu(3)-N(2)[i]	91.57(10)
O(3)-Cu(2)-O(5)	176.28(13)	O(9)-Cu(3)-N(2)[i]	97.49(11)
O(8)-Cu(3)-N(2)[i]	95.14(10)	O(7)-Cu(3)-N(2)[i]	89.15(10)

[i] Symmetry Code: *x*+1, *y*, *z*
[ii] Symmetry Code: *x*-1, *y*, *z*

**Specific details for {[(Cu$_3$(L^2)$_3$)(bipy)(THF)]·2.75THF}$_n$**

There are 2.75 disordered THF molecules within the asymmetric unit. The O(4T) containing THF is 0.5 occupancy, the O(2T)- and O(7T)-containing molecules represent one whole THF modelled over two positions (0.6 and 0.4 occupancies respectively), the O(3T)-containing THF is 0.75 occupancy and the O(5T)- and O(6T)-containing THF molecules represent one 0.5 occupancy THF modelled over two positions. Hydrogen atoms were not modelled on carbon atoms with 0.25 occupancy.   The ethyl group beginning at C(46) is disordered with two positions modelled giving a total occupancy of 1. Part of one of the other β-diketonate ligands is also disordered over two positions, again modelled with each of the total occupancies of C(13)-C(16) equaling one. The amount of disorder present in the structure is significant and the resulting high U_{eq} min/max ratios, reflect the presence of this disorder in both solvent and propyl groups and the poor quality of diffraction data obtained from the sample. This can probably be attributed to solvent loss during the mounting process prior to quenching in the cryostream at 150 K.

Table S2. Selected Bond Lengths (Å) and Angles (°) for [{[(Cu$_3$(L^2)$_3$)(bipy)(THF)]·2.75THF}$_n$

Cu(1)-O(11)	1.925(2)	Cu(1)-N(1)	2.314(3)
Cu(1)-O(12)	1.934(2)	Cu(2)-O(3)	1.916(2)
Cu(1)-O(2)	1.937(2)	Cu(2)-O(4)	1.919(3)
Cu(1)-O(1)	1.941(2)	Cu(2)-O(6)	1.922(2)
Cu(3)-O(7)	1.942(2)	Cu(2)-O(5)	1.931(2)

Figure S2. ORTEP plot of the asymmetric unit of $\{[(Cu_3(\mathbf{L}^2)_3)(bipy)(THF)]\cdot 2.75THF\}_n$ shown with 50% probability ellipsoids. THF solvate molecules and lower population disordered positions removed for clarity.
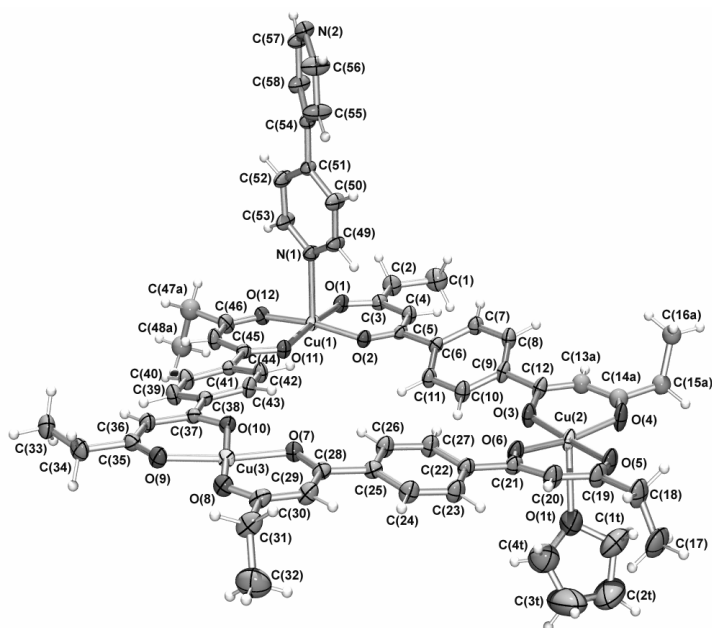
Table S3. Selected Bond Lengths (Å) and Angles (°) for

{[Cu$_3$(L^2)$_3$(bipy)(THF)]·bipy·0.75THF}$_n$

Cu(1)-O(1)	1.941(2)	Cu(2)-O(4)	1.935(2)
Cu(1)-O(2)	1.942(2)	Cu(2)-O(6)	1.945(2)
Cu(1)-O(11)	1.943(2)	Cu(2)-N(2)^i	2.314(3)
Cu(1)-O(12)	1.947(2)	Cu(3)-O(10)	1.918(2)
Cu(1)-N(1)	2.262(3)	Cu(3)-O(7)	1.920(2)
Cu(2)-O(3)	1.927(2)	Cu(3)-O(8)	1.920(2)
Cu(2)-O(5)	1.927(2)	Cu(3)-O(9)	1.923(2)
		Cu(3)-O(1T)	2.416(3)
O(1)-Cu(1)-O(2)	91.97(9)		
O(1)-Cu(1)-O(11)	160.90(10)	O(11)-Cu(1)-N(1)	93.84(10)
O(2)-Cu(1)-O(11)	87.00(9)	O(12)-Cu(1)-N(1)	92.94(10)
O(1)-Cu(1)-O(12)	86.75(9)	O(3)-Cu(2)-O(5)	172.30(10)
O(2)-Cu(1)-O(12)	175.90(10)	O(3)-Cu(2)-O(4)	93.35(9)
O(11)-Cu(1)-O(12)	92.93(9)	O(5)-Cu(2)-O(4)	86.06(9)
O(1)-Cu(1)-N(1)	105.25(10)	O(3)-Cu(2)-O(6)	87.95(9)
O(2)-Cu(1)-N(1)	91.15(10)	O(5)-Cu(2)-O(6)	92.11(9)
O(5)-Cu(2)-N(2)^i	101.06(10)	O(4)-Cu(2)-O(6)	175.73(10)
O(3)-Cu(2)-N(2)^i	86.63(9)	O(4)-Cu(2)-N(2)^i	96.08(10)
O(10)-Cu(3)-O(8)	174.63(11)	O(6)-Cu(2)-N(2)^i	88.06(10)
O(7)-Cu(3)-O(8)	93.62(10)	O(10)-Cu(3)-O(7)	85.23(10)
O(7)-Cu(3)-O(9)	175.01(11)	O(8)-Cu(3)-O(1T)	93.00(10)
O(8)-Cu(3)-O(9)	87.75(10)	O(9)-Cu(3)-O(1T)	96.22(10)
O(10)-Cu(3)-O(1T)	92.21(10)	O(7)-Cu(3)-O(1T)	88.50(10)

^{i} Symmetry Code: *x, y+1, z*
^{ii} Symmetry Code: *x, y-1, z*
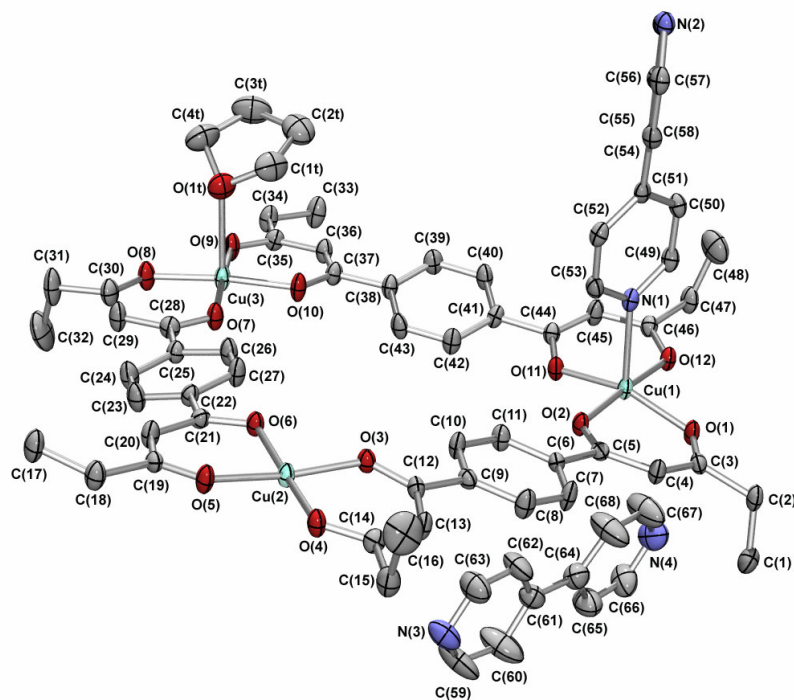
Figure S3. ORTEP plot of the asymmetric unit of
$\{[Cu_3(\mathbf{L^2})_3(bipy)(THF)]\cdot bipy\cdot0.75THF\}_n$ shown with 50% probability ellipsoids. Solvate molecules, hydrogen atoms and lower population disordered positions removed for clarity.

Specific details for $\{[(Cu_3(\mathbf{L^1})_3)(pyz)]\cdot THF\}_n$

The crystals of this complex displayed poor diffraction properties, with broadening being evident. The crystal from which the data were collected proved to be a non-merohedral twin resulting in the data collected being poor. No absorption correction was carried out and data were indexed and refined against one orientation of the unit cell. Final BASF values were 0.11066, 0.36793, 0.14235 and 0.03148 respectively. Inconsistent temperature factors, relatively low bond precision, high U_{eq} min/max ratios, high electron

density residual peaks (1.722, -2.368 e⁻ Å⁻³) and high *R* factors are very likely due to the

twinning and the poor diffraction properties of the crystals. In addition, two of the six

ethyl groups are disordered, with one modelled over two positions and the other over

three, each with a total occupancy of one. There are some short H - H contacts, however,

these exist between atoms present in a region of disorder and are a result of that

modelling and are not true contacts.

Table S4. Selected Bond Lengths (Å) and Angles (°) for {[(Cu$_3$(L^1)$_3$)(pyz)]·THF}

Cu(1)-O(2)	1.923(4)	Cu(2)-O(3)	1.933(4)
Cu(1)-O(12)	1.927(4)	Cu(2)-O(5)	1.951(5)
Cu(1)-O(11)	1.931(4)	Cu(2)-O(4)	1.952(5)
Cu(1)-O(1)	1.936(4)	Cu(2)-N(2)^i	2.356(7)
Cu(1)-N(1)	2.317(6)	Cu(3)-O(8)	1.900(6)
Cu(2)-O(6)	1.928(5)	Cu(3)-O(7)	1.915(6)
Cu(3)-O(10)	1.931(5)	N(2)-Cu(2)^{ii}	2.356(7)
Cu(3)-O(9)	1.947(6)		
O(2)-Cu(1)-O(12)	173.9(2)	O(11)-Cu(1)-N(1)	91.3(2)
O(2)-Cu(1)-O(11)	86.09(17)	O(1)-Cu(1)-N(1)	99.3(2)
O(12)-Cu(1)-O(11)	92.96(18)	O(6)-Cu(2)-O(3)	86.0(2)
O(2)-Cu(1)-O(1)	92.73(17)	O(6)-Cu(2)-O(5)	93.0(2)
O(12)-Cu(1)-O(1)	87.09(18)	O(3)-Cu(2)-O(5)	175.1(2)
O(11)-Cu(1)-O(1)	169.4(2)	O(6)-Cu(2)-O(4)	172.0(2)
O(2)-Cu(1)-N(1)	90.97(19)	O(3)-Cu(2)-O(4)	93.3(2)
O(12)-Cu(1)-N(1)	95.1(2)	O(5)-Cu(2)-O(4)	87.1(2)
O(6)-Cu(2)-N(2)^i	94.1(2)	O(4)-Cu(2)-N(2)^i	93.8(2)
O(3)-Cu(2)-N(2)^i	90.7(2)	O(8)-Cu(3)-O(7)	94.2(3)
O(5)-Cu(2)-N(2)^i	94.1(2)	O(8)-Cu(3)-O(10)	177.6(2)
O(7)-Cu(3)-O(10)	86.7(2)	O(7)-Cu(3)-O(9)	170.3(2)
O(8)-Cu(3)-O(9)	86.1(3)	O(10)-Cu(3)-O(9)	92.6(3)

^{i} Symmetry Code: *x*+1*, y, z*
^{ii} Symmetry Code: *x*-1*, y, z*
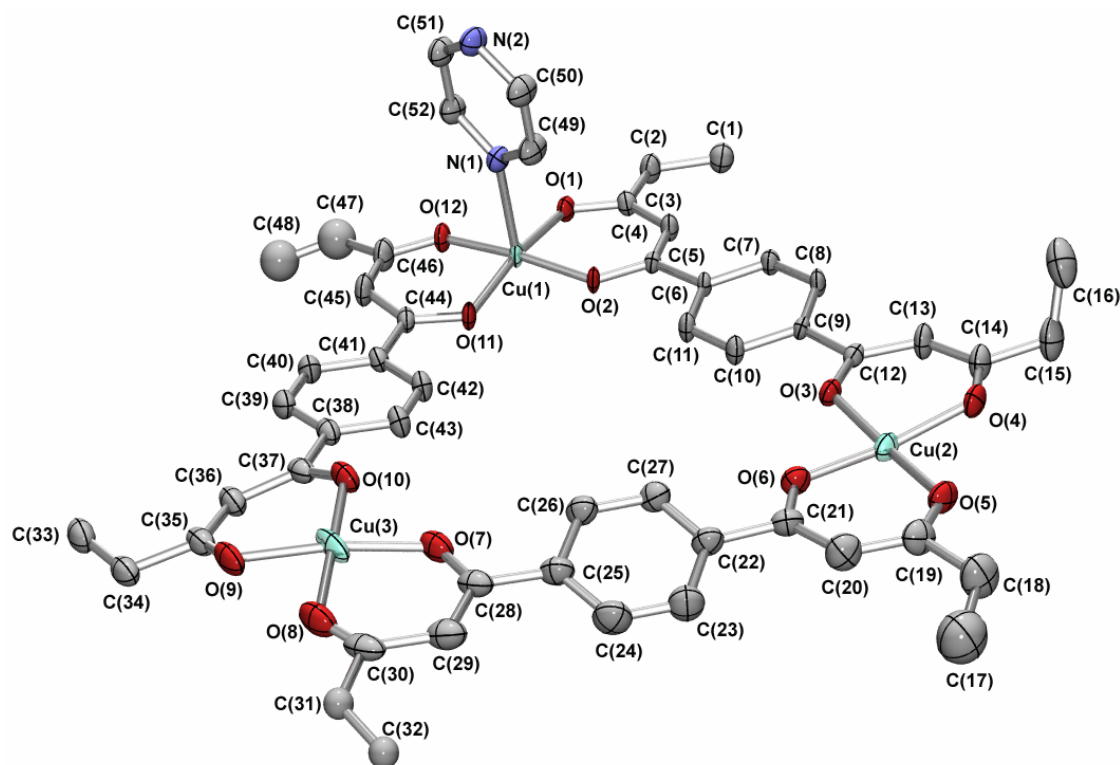
Figure S4. ORTEP plot of the asymmetric unit of $\{[(Cu_3(\mathbf{L^1})_3)(pyz)]\cdot THF\}_n$ shown with 30% probability ellipsoids. Solvate molecules, hydrogen atoms and lower population disordered positions removed for clarity.

Specific details for $\{[(Cu_3(\mathbf{L^3})_3)(dabco)_3]\cdot 3Et_2O\}_n$

The structure crystallised in the monoclinic space group $P2_1/m$ with β very close to 90° (90.130(2)°) and proved to be a twin with a two-fold rotation about a, thus emulating orthorhombic symmetry with space group Pmmn.[1] The twinning was accounted for by the use of the appropriate twin law in SHELXL-97[2] resulting in a significant decrease in the R factor. Interestingly, ROTAX found two pseudo-merohedral twin laws corresponding closely to the twin law employed, however, neither of them improved the refinement to the extent of the one used.[3,4] The major twin fraction refined to occupancy of 0.72 and no absorption correction was carried out. The structure is also significantly

disordered. Each of the tertiary butyl groups of the ligands are disordered and were modelled in two positions as were the phenyl rings contained within the ligands. FLAT restraints were applied to these disordered rings. The dabco ligands are significantly rotationally disordered, one modelled in two positions and the other in four each with a total occupancy of one with some of the carbon atoms lying on special positions. Despite modelling 2.5 diethyl ether solvent molecules per unit cell, there was a significant amount of residual electron density which could not be effectively modelled, possibly due to solvent loss during the mounting process (despite rapid handling at 200 K before quenching at 150K). The squeeze function of PLATON[5] was employed to remove the contribution of this electron density from the data. PLATON estimated the electron count to be 263 per unit cell which corresponds to approximately 3.5 diethyl ether molecules per unit cell, or 1.75 per molecule. Elemental analysis after prolonged drying showed no residual solvent, which is consistent with the apparent loss of solvent experienced during the mounting process.

Table S5. Selected Bond Lengths (Å) and Angles (°) for

$\{[(Cu_3(L^3)_3)(dabco)_3] \cdot 3Et_2O\}_n$

| O(1)-Cu(1) | 1.939(3) | O(5)-Cu(1) | 1.946(3) |

O(2)-Cu(1)	1.940(3)	O(6)-Cu(1)	1.940(3)
O(3)-Cu(2)	1.941(3)	Cu(2)-O(3)^i	1.941(3)
O(4)-Cu(2)	1.945(3)	Cu(2)-O(4)^i	1.945(3)
N(1)-Cu(1)	2.491(3)	Cu(2)-N(3)	2.501(3)
Cu(1)^{ii}-N(2)	2.506(3)	Cu(2)^{ii}-N(4)	2.515(3)
O(6)-Cu(1)-O(2)	87.72(11)	O(3)^i-Cu(2)-O(3)	87.40(15)
O(6)-Cu(1)-O(1)	179.33(13)	O(3)^i-Cu(2)-O(4)	179.94(14)
O(2)-Cu(1)-O(1)	91.91(11)	O(3)-Cu(2)-O(4)	92.56(11)
O(6)-Cu(1)-O(5)	92.31(12)	O(3)^i-Cu(2)-O(4)^i	92.56(11)
O(2)-Cu(1)-O(5)	179.81(14)	O(3)-Cu(2)-O(4)^i	179.94(14)
O(1)-Cu(1)-O(5)	88.07(12)	O(4)-Cu(2)-O(4)^i	87.48(16)

[i] Symmetry Code: *x, -y+1/2, z*

[ii] Symmetry Code: *-x, -y, -z*
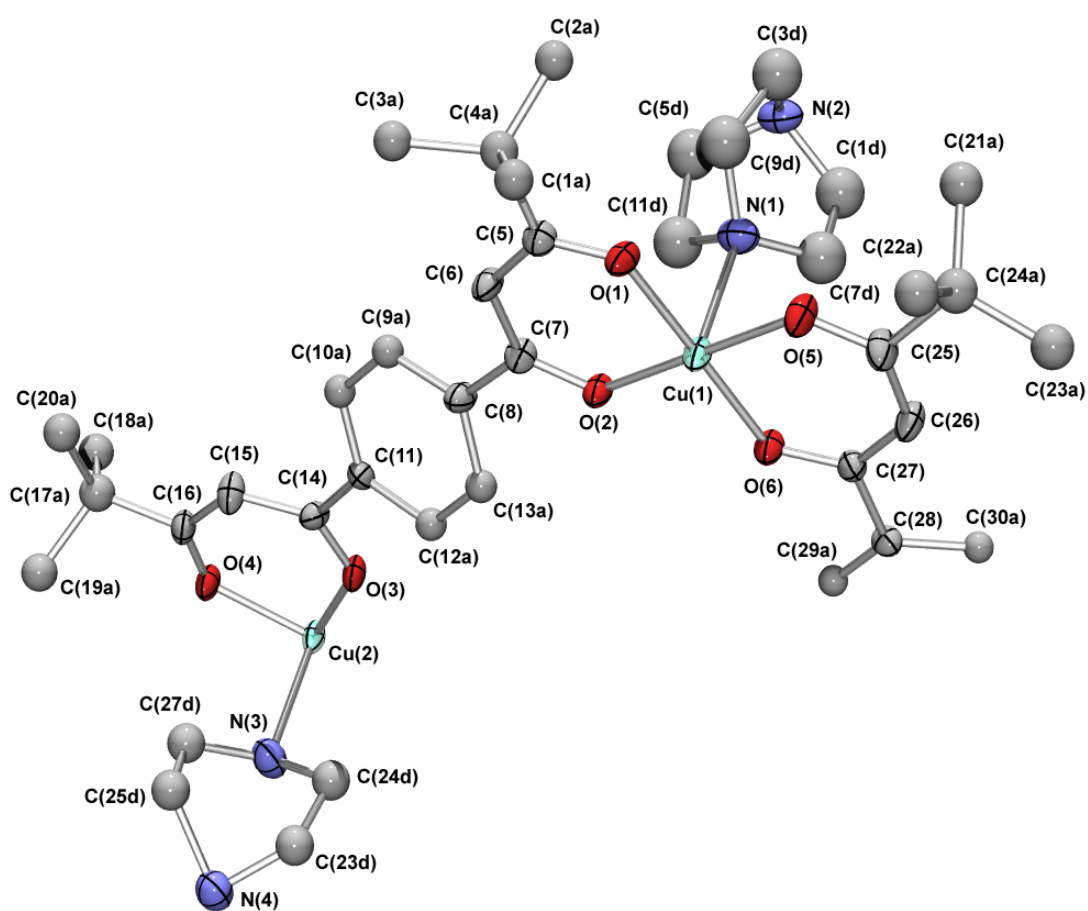
Figure S5. ORTEP plot of the asymmetric unit of $\{[(Cu_3(\mathbf{L^3})_3)(dabco)_3]\cdot 3Et_2O\}_n$ shown with 50% probability ellipsoids. Solvate molecules, hydrogen atoms and lower population disordered positions removed for clarity.

Specific details for {[Cu₃(L³)₃](hmt)}ₙ

Carbon atoms C(1)-C(5) and C(16)-C(18) are disordered, with the former modelled over

two positions (A,B) and the later over three (A,B,C). Each atom is modelled with a

combined occupancy of one. A suitable error model for the absorption correction could

not be found with SADABS[6] and consequently no correction was applied. The absolute

configuration was assigned using anomalous dispersion affects from the diffraction

pattern and was confirmed by the the Flack parameter which refined to 0.00(2).[7]

Table S6. Selected Bond Lengths (Å) and Angles (°) for {[Cu₃(L³)₃](hmt)}ₙ

O(1)-Cu(1)	1.931(4)	O(4)-Cu(1)^i	1.942(3)
O(2)-Cu(1)	1.924(3)	Cu(1)-O(3)^{ii}	1.940(3)
O(3)-Cu(1)^i	1.940(3)	Cu(1)-O(4)^{ii}	1.942(3)
O(2)-Cu(1)-O(1)	92.01(14)	O(3)^{ii}-Cu(1)-O(4)^{ii}	91.98(14)
O(2)-Cu(1)-O(3)^{ii}	88.42(14)	O(2)-Cu(1)-N(1)	99.59(14)
O(1)-Cu(1)-O(3)^{ii}	171.24(16)	O(1)-Cu(1)-N(1)	92.21(16)
O(2)-Cu(1)-O(4)^{ii}	168.20(15)	O(3)^{ii}-Cu(1)-N(1)	96.35(14)
O(1)-Cu(1)-O(4)^{ii}	85.82(14)	O(4)^{ii}-Cu(1)-N(1)	92.09(14)

^{i} Symmetry Code: *z*-1, *x*, *y*+1

^{ii} Symmetry Code: *y*, *z*-1, *x*+1
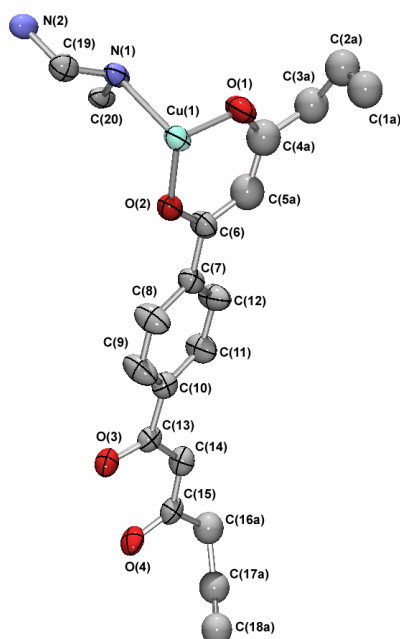
Figure S6. ORTEP plot of the asymmetric unit of $\{[Cu_3(\mathbf{L^3})_3](hmt)\}_n$ shown with 50% probability ellipsoids. Hydrogen atoms and lower population disordered positions removed for clarity.

References

1   S. Parsons, *Acta Cryst.* 2003, D**59**, 1995-2003.

2   G. M. Sheldrick, *SHELX-97: Programs for Crystal Structure Analysis*, University of Göttingen, Institüt für Anorganische Chemieder Universität, Tammanstrasse 4, D-3400 Göttingen, Germany, 1997.

3   R.I. Cooper, R.O. Gould, S. Parsons, D. J. Watkin, *J. Appl. Cryst.*, 2002, **35**, 168-174.

4   WinGX-32: System of programs for solving, refining and analysing single crystal X-ray diffraction data for small molecules, L. J. Farrugia, *J. Appl. Cryst.*, 1999 32, 837.

5   PLATON, A. L. Spek, *Acta Cryst.*, 1990, **A46**, C-34.

6   G. M. Sheldrick, SADABS: empirical absorption and correction software. University of Göttingen, Institüt für Anorganische Chemie der Universität, Tammanstrasse 4, D-3400 Göttingen, Germany, 1999.

7   H. D. Flack, *Acta Cryst.*, 1983. **A39**, 876-881.